Journal of Tissue Engineering
Volume 9: 1–8

DOI: 10.1177/2041731418766418
journals.sagepub.com/home/tej
SAGE

A 3D-printed passive ultrasound phase-interference compensator for reduced wave degradation in cancellous bone – an experimental study in replica models

Christian M Langton[1,2,3], Saeed M AlQahtani[1,2,4] and Marie-Luise Wille[1,2]

Abstract

The current 'active' solution to overcome the impediment of ultrasound wave degradation associated with transit-time variation in complex tissue structures, such as the skull, is to vary the *transmission delay* of ultrasound pulses from individual transducer elements. This article considers a novel 'passive' solution in which constant transit time is achieved by propagating through an additional material layer positioned between the ultrasound transducer and the test sample. To test the concept, replica models based on four cancellous bone natural tissue samples and their corresponding passive ultrasound phase-interference compensator were 3D-printed. Normalised broadband ultrasound attenuation was used as a quantitative measure of wave degradation, performed in transmission mode at a frequency of 1 MHz and yielding a reduction ranging from 57% to 74% when the ultrasound phase-interference compensator was incorporated. It is suggested that the passive compensator offers a broad utility and, hence, it may be applied to any ultrasound transducer, of any complexity (single element or array), frequency and dimension.

Keywords

Three-dimensional printing, transcranial ultrasound, wave degradation, transit time

Date received: 27 August 2017; accepted: 26 February 2018

Introduction

As an ultrasound wave propagates through a complex composite structure such as skull tissue, variations in both thickness and composition lead to variations in both transit time and amplitude; thereby creating wave degradation, schematically illustrated in Figure 1. The term 'wave degradation' is a qualitative term indicating that the 'output' and 'input' signals are observably dissimilar; this may be quantified by both time-domain (pulse-length, amplitude) and frequency-domain (phase, amplitude) analyses.

Several approaches have previously been considered to overcome the impediment of ultrasound wave degradation associated with transcranial propagation. In 1975, Phillips et al.[1] described an 'active' signal processing approach to address the significant time shifts related to variations in skull thickness over the aperture of conventional ultrasound transducers, as illustrated in Figure 2. By utilising a multi-element array of equally spaced small-width elements, transmission delays were varied to compensate for differences in tissue thickness and composition. To determinate the individual element delay, a pulse-echo technique was developed. An

[1]Science and Engineering, Queensland University of Technology, Brisbane, QLD, Australia
[2]Institute of Health and Biomedical Innovation, Queensland University of Technology, Brisbane, QLD, Australia
[3]Laboratory of Ultrasonic Electronics, Doshisha University, Kyotanabe, Japan
[4]University College in Al Jamoom, Umm Al-Qura University, Mecca, Saudi Arabia

Corresponding author:
Christian M Langton, Institute of Health and Biomedical Innovation, Queensland University of Technology, 60 Musk Avenue, Kelvin Grove, 4059 QLD, Australia.
Email: christian.langton@qut.edu.au

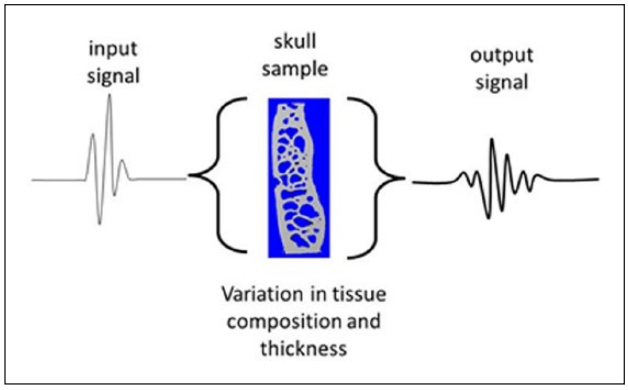

Figure 1. The problem: inherent transit-time variation through a skull sample creates wave degradation.

alternative approach was also reported, describing phase variations across the transducer as a mathematical expression, implemented via non-linear signal processing.

In 1996, Thomas and Fink[2] described the potential application of time-reversal mirrors (TRMs) made of large transducer arrays aimed at allowing the incident field to be sampled, time reversed and re-emitted. In 2009, a numerical computation was described by Marquet et al.[3] to determine the impulse response relating the targeted location and the ultrasound therapeutic array; this was then time-reversed and transmitted experimentally by a therapeutic array.

The thickness profile of the skull may be measured from X-ray computed tomography (CT) images. These data may be incorporated within a simulation software program to first predict the phase-shifts induced by the skull and, second, to control the phase and amplitude of each element within a spherical array.[4] This approach has been applied by Clement and Hynynen[5,6] to a propagation model based on a projection algorithm in the wave-vector frequency domain. In 2001, Pernot et al.[7] suggested that efficient non-invasive therapy would require adaptive focusing to account for the acoustical properties of the skull, experimentally validating a three-dimensional (3D) finite-difference simulation yielding computed ultrasound wavefronts through the skull. A passive micro-bubble-derived aberration correction technique has recently been described;[8] a comparison of actual and predicted transit times at each element of a hemispherical array was again used to determine the required transmission delays.

The 'active' approach is now widely utilised within a number of proprietary high-intensity focused ultrasound (HIFU) clinical systems.

From a diagnostic imaging perspective, the conventional clinical approach is to utilise the 'acoustic window' within the temporal bone of the skull that exhibits relatively low levels of wave degradation. As with the therapeutic perspective, improvement in acoustic window propagation has been reported through implementation of 'active' transmission-delay techniques.[9]

A novel 'passive' approach has recently been proposed in which constant transit time may be achieved by incorporating an additional material layer.[10] Hence, this ultrasound phase-interference compensator (UPIC) provides a solution based on variable *propagation* rather than variable *transmission* of ultrasound pulses. It is hypothesised that the 'passive' UPIC concept offers a broad utility, where it may be applied to single element and linear-array ultrasound transducers of any frequency and dimension, along with utility to both pulse-echo-mode diagnostic imaging and transmission-mode therapeutic transcranial applications.

Ultrasound transit time spectroscopy and the UPIC concept

Langton[11] has previously proposed that propagation of an ultrasound wave through a complex composite sample, such as cancellous bone, may be considered as an array of parallel sonic rays. For a complex porous sample replicating cancellous bone, of total thickness d, composed of solid (ultrasound velocity v_s) and liquid (ultrasound velocity v_l), the minimum (t_{min}) and maximum (t_{max}) transit times will be d/v_s and d/v_l, respectively, describing the entire solid and liquid, respectively. For a sonic ray propagating through a combination of solid and liquid media of overall thicknesses d_s and d_l, respectively, the total transit time will be $d_s/v_s + d_l/v_l$, noting that there may be a summation of several segments, for example, solid filaments and liquid cavities. We may therefore create a transit-time spectrum, ranging from t_{min} to t_{max}, describing the proportion $P(t_i)$ of sonic rays having a particular transit-time (t_i), which corresponds to a spatial proportion of the receive transducer aperture. The maximum value of $P(t_i)$ is unity, when all sonic rays have the same transit time, examples being entire solid, entire liquid or a combination of these that is consistent over the receive transducer aperture.

We may meet the condition of constant total transit time (t_o) simply by incorporating a temporal 'inverse' of the test sample, where solid is replaced by liquid, and vice versa, as schematically shown in Figure 3.

The sonic-ray propagation concept considers the total transit time through composite tissues, where internal structure is manifested as lateral heterogeneity. Reflection and refraction are considered to be secondary phenomena. The validity of the concept is supported by its accurate estimation of bone volume fraction in structurally complex human cancellous bone samples in vitro,

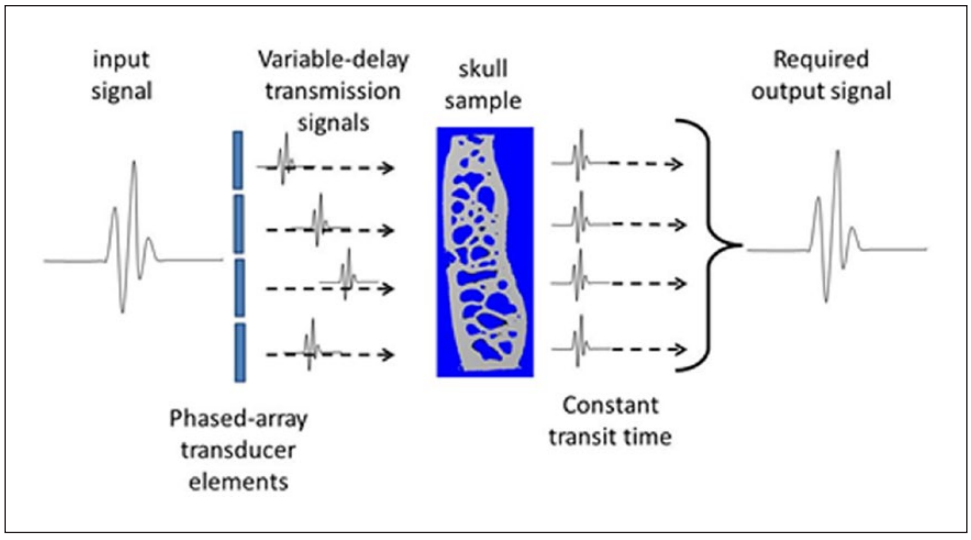

Figure 2. The current 'active' solution: inherent transit-time variation through a skull sample is compensated by varying the transmission delay of ultrasound pulses from individual transducer elements.

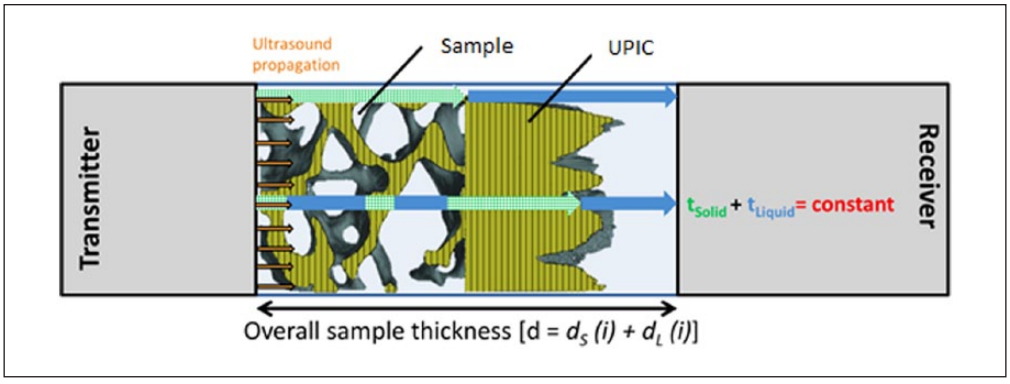

Figure 3. UPIC concept: inherent transit-time variation through a porous composite sample is compensated by varying the propagation time of sonic rays (i) through an additional material layer.

reporting an R^2 of 88.5% against the X-ray μCT gold standard.[12]

Methodology

Samples

The study utilised externally sourced microCT-derived binary data sets (bone/void) from four 4-mm cuboid human natural tissue cancellous bone samples, the anatomical sites being femoral head (FH), lumbar spine (LS), calcaneus (CA) and iliac crest (IC). The uni-axial voxel dimension was 14 μm (28 μm for calcaneus). A cylindrical volume of interest was extracted from each sample, equivalent to a natural tissue diameter of 2.6 mm. The voxel dimensions were then isotropically magnified by a factor of 7.3, the sample diameter thereby equalling the receive transducer aperture diameter of 19 mm.

By manipulating the voxelised data, two designs were created for each cancellous bone sample using custom-written MATLAB programs (MathWorks Inc., Natick, MA, USA):

1. Core: cylindrical replica of natural tissue cancellous bone samples derived from binary microCT data.
2. Combined: the length of cavities along the cylinder, parallel to the direction of ultrasound propagation, for each voxel position (xy) over the flat circular surface were summed and converted into a solid design representing the UPIC. The cancellous bone core and solid UPIC were axially aligned, as schematically shown in Figure 3, to create a 'combined' model.

The two designs for each of the four cancellous bone samples were converted into STL (stereolithography) file

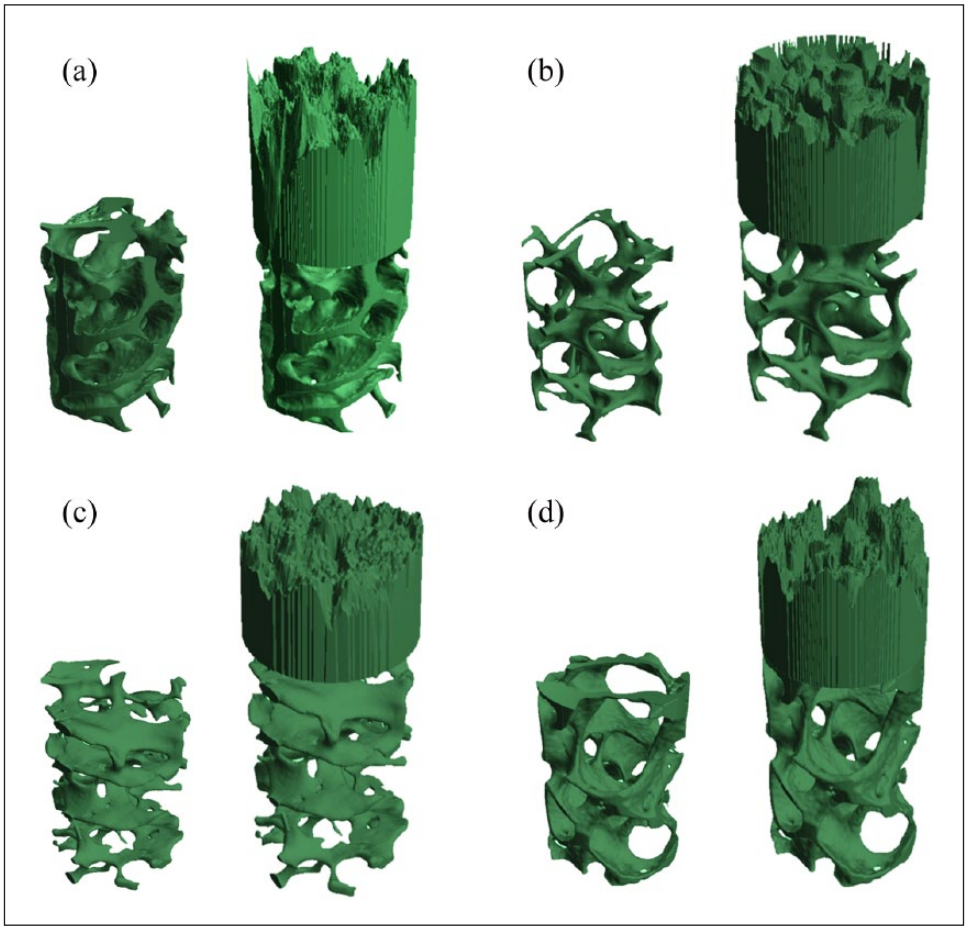

Figure 4. 3D designs of the core and combined models of (a) femoral head, (b) lumbar spine, (c) calcaneus and (d) iliac crest samples.

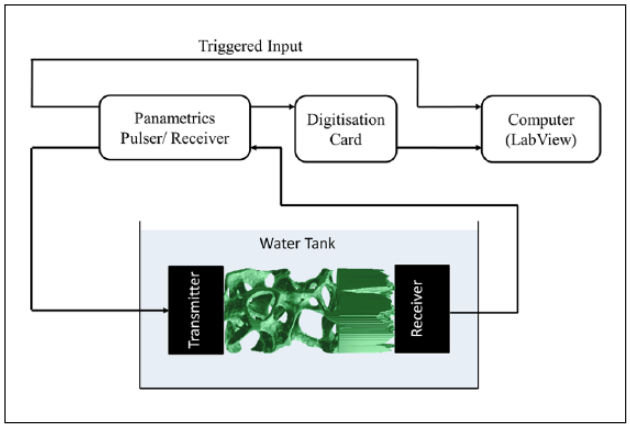

Figure 5. Schematic diagram of the experimental set-up.

format and 3D-printed in VisiJet FTX Green material using a ProJet1200 Micro-SLA Printer (3D Systems Inc., Rock Hill, SC, USA). Figure 4 shows the 3D designs of the two models for each of the four cancellous bone natural tissue samples.

Ultrasound measurements

Two 1-MHz, 19-mm active-element diameter, broadband planar-circular ultrasound transducers (Harisonics model I7-0112-G, Olympus NDT Inc., Waltham, MA, USA) were aligned co-axially at a fixed separation of 51.5 mm in a water bath at a temperature of 23°C ± 2.5°C. One transducer served as transmitter and the other as receiver. A pulser-receiver (Panametrics 5058PR, Olympus NDT Inc.) was used to provide the excitation spike (400 V with a pulse-width of 7 ns) and to amplify the receive signals. The radio-frequency (RF) output signal from the pulser-receiver was fed into a 14-bit digitiser card operating at 100 MHz sampling rate; 7000 samples were recorded corresponding to a measurement period of 70 μs. A schematic diagram of the experimental set-up is shown in Figure 5.

A reference signal was recorded for propagation through water alone; the received signal had a pulse length of 2.79 μs, a centre frequency of 0.811 MHz, with a −3 dB bandwidth of 0.61–1.07 MHz, providing a Q-value of 1.8.

Five repeat measurements were performed on each of the core and combined models. For each repeat measurement, the sample was remounted and axially rotated by 90°. Furthermore, indistinguishable signals were obtained when transmit and receive transducers were swapped, thereby changing the direction of ultrasound propagation through the samples.

Signal analysis

Solid volume normalised broadband ultrasound attenuation (svnBUA; dB/MHz/cm^3) was utilised as the quantitative parameter for phase-interference induced wave degradation, based on the experimental evidence that its primary attenuation mechanism dependence in cancellous bone is phase-interference;[13] hence, the authors envisage that a reduction in phase-interference will result in a corresponding reduction in the svnBUA value. svnBUA describes the linear increase in ultrasound attenuation with frequency over the range of 200–600 kHz, divided by the solid volume of each model.[14] BUA measurement of cancellous bone samples, where the volume fraction is nominally consistent throughout, is conventionally normalised by thickness (cm). Noting that a UPIC is essentially a complex-shaped solid, BUA was divided by the total volume of 3D-print material within each test model (cm^3), thereby normalising for the volume fraction of bone and UPIC.

Results

The ultrasound velocity, attenuation coefficient and svnBUA of the 3D-print material, using a solid cylindrical sample, were measured at 1 MHz, being 2430 ± 10 m/s, 42.1 ± 0.2 Np/m and 1.34 ± 0.06 dB/MHz/cm^3, respectively. Its density was experimentally measured to be 1.2 ± 0.15 g/cm^3.

Figures 6 and 7 show experimentally recorded waveforms and svnBUA data (mean ± standard deviation) for repeat measurements of core and corresponding combined models for each of the four cancellous bone samples; the percentage reduction in wave degradation provided by incorporation of the UPIC, calculated as svnBUA[(core − combined)]/svnBUA(core), is provided in Table 1.

Discussion

This article considered a novel means aimed at significantly reducing wave degradation associated with ultrasound propagation through the complex porous composite of cancellous bone; a primary component of skull bone tissue. By creating an environment of constant transit time, through the combination of a replica cancellous bone sample and its temporal inverse, UPIC thereby offers the potential to reduce ultrasound wave degradation through complex tissues. Percentage improvements in the fidelity of ultrasound propagation, ranging from 57% to 74%, as defined by the quantitative measure of broadband ultrasound attenuation, are reported.

As with the current ‘active’ approach, for clinical implementation, it is envisaged that calculation of a specific UPIC design will be based on X-ray CT-scan data and analysis, from which the bespoke physical UPIC device would be 3D-printed. The accuracy of the UPIC concept will therefore be dependent on a number of factors, including the spatial resolution of both the CT-scan data and the 3D-printing process, along with the ultrasound properties of the UPIC material. A significant benefit of the ‘passive’ UPIC concept has recently been reported, demonstrating that ultrasound wavefront correction may be implemented for features that are smaller than the dimensions of the ultrasound transducer element(s), being the primary spatial resolution limiting factor for the current ‘active’ approach.[15] The passive UPIC concept offers a broad utility and the authors consider that it may be applied to single-element and linear-array ultrasound transducers of any frequency and dimension. Future work should determine UPIC’s performance associated with utility of a concave transducer and/or a curved sample surface such as the skull.

It is envisaged that the clinical utility of UPIC will be associated with patients suffering from severe neurological (Alzheimer’s, Parkinson’s, etc.) or oncology (tumour) conditions, and hence, clinical X-ray CT (or magnetic resonance imaging (MRI)) scan data will be available to facilitate a patient-specific UPIC design.

The main limitation of this study is that magnified replica models of natural tissue cancellous bone samples were used. Future work should consider natural tissue samples, including those from the skull. Furthermore, a comparison of passive and active approaches should be performed, comparing spatial maps of the transmitted field, with and without the passive compensator incorporated. The current ‘active’ approach also incorporates compensation for absorption variability, implemented through controlled variation of the excitation signal amplitude applied to each individual ultrasound transducer. Noting that the passive compensator implemented within this study is also the spatial-inverse of the test sample, the total absorption experienced by each sonic ray will be constant when they are combined, again warranting further consideration.

Conclusion

This article considered a novel solution to overcome the impediment of ultrasound wave degradation associated

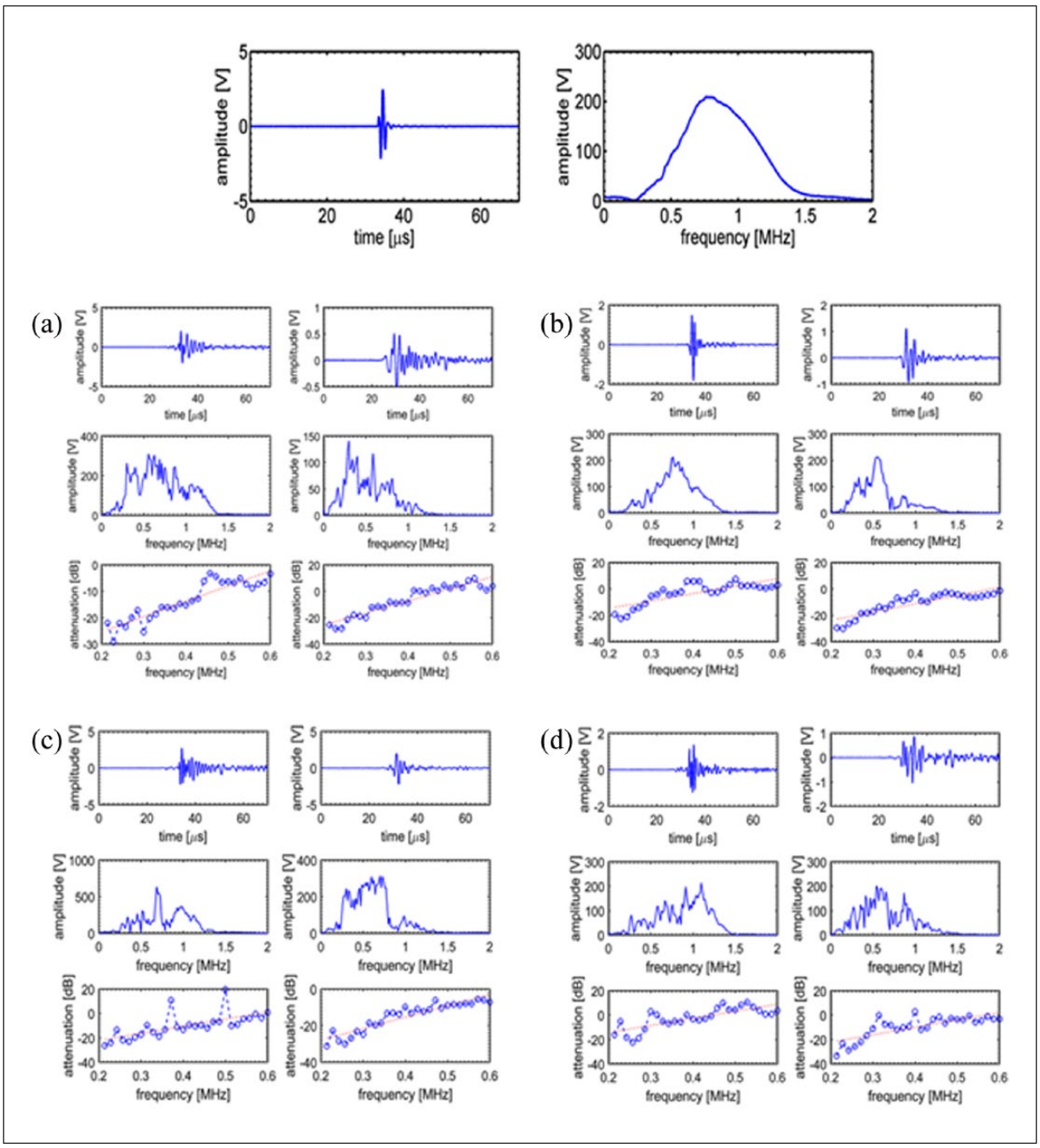

Figure 6. Row 1: time-domain ultrasound signal and corresponding frequency-domain spectrum for water alone. Rows 2 and 3: the two columns for each sample ((a) FH, (b) LS, (c) CA and (d) IC) indicate core and combined samples, respectively. The three rows for each sample, respectively, represent the time-domain signal, the frequency-domain spectrum and a plot of attenuation versus frequency, from which the BUA value was calculated

with transit-time variation, by varying the *propagation* time through an additional material layer, the passive UPIC being a temporal inverse of the test sample. A reduction in ultrasound wave degradation ranging from 57% to 74% was observed for replica models of cancellous bone samples when the UPIC was incorporated. It is suggested that the UPIC concept offers a broad utility, where it may be applied to any ultrasound transducer, of any complexity (single element or array), frequency and dimension. Future work should consider natural tissue samples, including those from the skull.

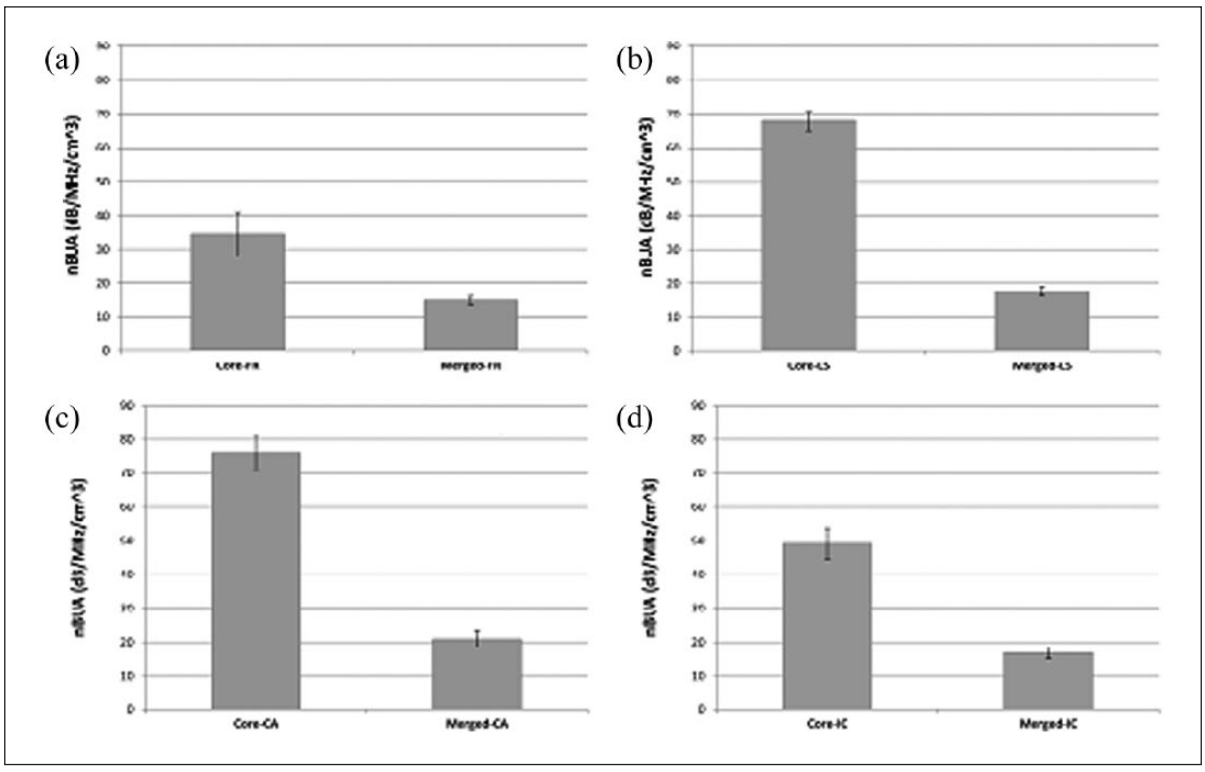

Figure 7. svnBUA analysis including standard deviation for core and combined models for each of the four cancellous bone samples: (a) femoral head, (b) lumbar spine, (c) calcaneus and (d) iliac crest.

Table 1. svnBUA data for core and combined models along with percentage reduction, representing the improvement in ultrasound wave propagation provided by UPIC.

Sample	Core svnBUA (dB/MHz/cm^3)	Combined svnBUA (dB/MHz/cm^3)	UPIC improvement (%)
Femoral head	34.2 ± 6.6	14.6 ± 1.2	57.3 ± 6.7
Lumbar spine	67.8 ± 2.9	17.4 ± 1.5	74.3 ± 3.3
Calcaneus	76.2 ± 5.2	21 ± 2.4	72.4 ± 5.7
Iliac crest	49.2 ± 4.6	16.7 ± 1.8	66.1 ± 5.0
Average			67.5 ± 10.7

svnBUA: solid volume normalised broadband ultrasound attenuation; UPIC: ultrasound phase-interference compensation.

Acknowledgements

The authors wish to acknowledge Dr Bert Van Rietbergen (Eindhoven University of Technology, Netherlands) for providing the three-dimensional (3D) data sets, the support provided by Ms Melissa Johnston associated with creation of the 3D-printed models, Mr Ali Alomari for provision of his MATLAB BUA code and Professor Scott Wearing for helpful comments on the manuscript.

Declaration of conflicting interests

The author(s) declared no potential conflicts of interest with respect to the research, authorship and/or publication of this article.

Funding

The author(s) received no financial support for the research, authorship and/or publication of this article.

References

1. Phillips DJ, Smith SW, von Ramm OT, et al. Sampled aperture techniques applied to B-mode echoencephalography. In: Booth N. (eds) Acoust Hologr, Sprienger, Boston, MA: *Acoust Hologr* 1975; 103–120.
2. Thomas JL and Fink MA. Ultrasonic beam focusing through tissue inhomogeneities with a time reversal mirror: application to transskull therapy. *IEEE T Ultrason Ferr* 1996; 43(6): 1122–1129.
3. Marquet F, Pernot M, Aubry JF, et al. Non-invasive transcranial ultrasound therapy based on a 3D CT scan: protocol validation and in vitro results. *Phys Med Biol* 2009; 54(9): 2597–2613.
4. Hynynen K and Sun J. Trans-skull ultrasound therapy: the feasibility of using image-derived skull thickness information to correct the phase distortion. *IEEE T Ultrason Ferr* 1999; 46(3): 752–755.

5. Clement GT and Hynynen K. A non-invasive method for focusing ultrasound through the human skull. *Phys Med Biol* 2002; 47(8): 1219–1236.
6. Clement GT and Hynynen K. Correlation of ultrasound phase with physical skull properties. *Ultrasound Med Biol* 2002; 28(5): 617–624.
7. Pernot M, Aubry JF, Tanter M, et al. Experimental validation of 3D finite differences simulations of ultrasonic wave propagation through the skull. In: *Proceedings of the 2001 IEEE ultrasonics symposium* (ed DE Yuhas and SC Schneider), Atlanta, GA, 7–10 October 2001, vols 1 and 2, pp. 1547–1550. New York: IEEE.
8. O'Reilly MA and Hynynen K. A super-resolution ultrasound method for brain vascular mapping. *Med Phys* 2013; 40(11): 110701.
9. Ivancevich NM, Pinton GF, Nicoletto HA, et al. Real-time 3-D contrast-enhanced transcranial ultrasound and aberration correction. *Ultrasound Med Biol* 2008; 34(9): 1387–1395.
10. Langton CM. Passive twin-layer spatial-temporal phase-interference compensator for improved ultrasound propagation: a computer-simulation and experimental study in acrylic step-wedge samples. *Appl Acoust* 2018; 129: 181–189.
11. Langton CM. The 25th Anniversary of BUA for the assessment of osteoporosis: time for a new paradigm? *Proc IMechE, Part H: J Engineering in Medicine* 2011; 225(2): 113–125.
12. Alomari AH, Wille M-L and Langton CM. Bone volume fraction and structural parameters for estimation of mechanical stiffness and failure load of human cancellous bone samples; in-vitro comparison of ultrasound transit time spectroscopy and X-ray μCT. *Bone* 2018; 107: 145–153.
13. Wille M-L, AlQahtani SM and Langton CM. Is phase-interference the primary contributor to broadband ultrasound attenuation? A phantom study. In: *ANZORS 22nd annual scientific meeting*, Melbourne, VIC, Australia, 2016, 114;13-15 October: http://www.anzors.org.au/pdfs/2016-proceedings.pdf.
14. Langton CM, Palmer SB and Porter RW. The measurement of broadband ultrasonic attenuation in cancellous bone. *Eng Med* 1984; 13: 89–91.
15. Jones MWM, Shortell MP, Wille M-L, et al. Sub-transducer element spatial resolution ultrasound wavefront modification using passive twin-layer compensators. *Appl Acoust* 2018; 131: 129–133.